

## Au Nanotip as Luminescent Near-Field Probe

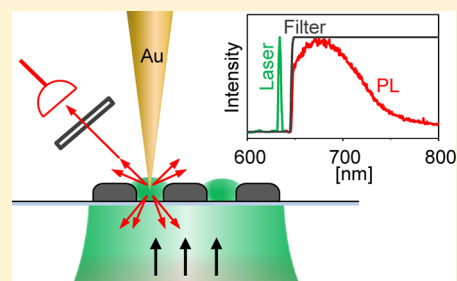
Sebastian Jäger,<sup>\*,†</sup> Andreas M. Kern,<sup>†</sup> Mario Hentschel,<sup>‡</sup> Regina Jäger,<sup>†</sup> Kai Braun,<sup>†</sup> Dai Zhang,<sup>†</sup> Harald Giessen,<sup>‡</sup> and Alfred J. Meixner<sup>\*,†</sup>

<sup>†</sup>Institute of Physical and Theoretical Chemistry, University of Tübingen, Auf der Morgenstelle 18, D-72076 Tübingen, Germany

<sup>‡</sup>4th Physics Institute and Research Center SCoPE, University of Stuttgart, Pfaffenwaldring 57, D-70569 Stuttgart, Germany

### **S** Supporting Information

**ABSTRACT:** We introduce a new optical near-field mapping method, namely utilizing the plasmon-mediated luminescence from the apex of a sharp gold nanotip. The tip acts as a quasi-point light source which does not suffer from bleaching and gives a spatial resolution of  $\leq 25$  nm. We demonstrate our method by imaging the near field of azimuthally and radially polarized plasmonic modes of nonluminescent aluminum oligomers.



**KEYWORDS:** One-photon photoluminescence, near-field microscopy, cylindrical vector beams, plasmonic oligomers, energy transfer

Imaging optical near fields of nano-objects has attracted significant experimental attention over the past few years. Several sophisticated methods were developed to reveal the shape and the localization of near fields, like near-field-induced polymerization<sup>1–3</sup> or various scanning tip-based techniques.<sup>4</sup> Some of these tip-based techniques use the luminescence of a point-like single emitter such as a single molecule to map the near fields of gold nano-objects.<sup>5</sup> While a single molecule is coming close to a point-like source, the stability of the fluorescence signal of a single molecule is weak, resulting in noisy images. Other point-like-emitter near-field probes are prepared in a complicated process by placing nanodiamonds with at least one nitrogen vacancy center at the apex of a glass-fiber tip.<sup>6</sup> Furthermore, the elastic scattering signal of single nano-objects has been used to detect local near fields, e.g., placing single 100 nm gold nanospheres on the apex of a glass-fiber tip.<sup>7</sup> Additionally, the scattering of a metallic or semiconductor tip with a tip radius of around 20 nm is used in scattering scanning near-field optical microscopy (SNOM).<sup>8,9</sup> However, the probes used in both scattering techniques are quite large and lead to significant perturbation of the near field of the investigated object. A further problem in scattering-mode SNOM arises from the fact that the signal is detected in the far field, where interference between the wave scattered from the probe and waves scattered from the confocally illuminated nanostructure obscures the signal. Apart from this, two-photon luminescence of a gold tip has been used to image the hot spots of gold particles upon illumination with a 120 fs laser at a wavelength of 780 nm.<sup>10</sup>

In this study we present a novel approach to investigate the near field of a plasmonic nano-object using the nonbleachable one-photon luminescence of a sharp gold tip with a tip radius of  $\leq 10$  nm. The photoluminescence (PL) of gold at visible wavelengths was first reported by Mooradian in 1969, shortly

after the invention of the laser.<sup>11</sup> These experiments were performed on plain bulk gold and showed an extremely weak luminescence yield of about  $10^{-10}$ . Experiments on rough gold island films with island sizes of 10–100 nm show a considerably larger luminescence quantum yield<sup>12</sup> going up to  $10^{-3}$  for gold nanorods.<sup>13</sup> While the PL signal from a plain gold surface is extremely weak, Au nanostructures exhibit a strong luminescence signal which is dependent on the local field intensity, e.g., in the near field of a gap nanoantenna.<sup>14,15</sup> The origin of the one-photon PL of gold nanoparticles is still a matter of active research and can be explained as the result of different processes, namely an interband electron hole pair recombination enhanced by the spectrally overlapping plasmon field as was suggested by Mohamed et al.<sup>13</sup> or by the direct inelastic radiative decay of a plasmon.<sup>16</sup> A recent investigation demonstrated fast interconversion between surface plasmons and hot electron hole pairs in optically excited nanoparticles, suggesting that the PL occurs via emission of a surface plasmon.<sup>17</sup> For the excitation power of the utilized 632.8 nm wavelength laser the intensity of gold PL is linear,  $I_{\text{PL}} = kI_{\text{loc}}(\vec{r})$  (see Supporting Information of ref 14). This linearity plus the stability of the gold PL signal makes sharp Au nanotips good candidates for the application as near-field sensors.

The measurement principle is illustrated in Figure 1. A single plasmonic nanostructure is centered into the focus of the laser beam and raster-scanned by an electrochemically etched sharp gold tip at a nanometer-scaled distance to the sample surface.<sup>18</sup> Both the photoluminescence signal of the gold tip and the topography of the sample are simultaneously acquired. An SEM

**Received:** April 2, 2013

**Revised:** June 20, 2013

**Published:** July 1, 2013

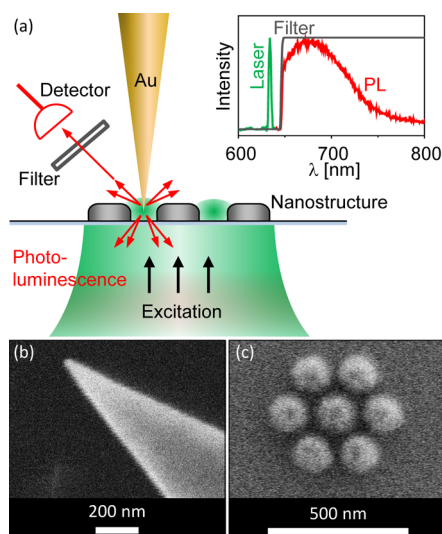


**Figure 1.** (a) Sketch of the measurement principle. The green excitation beam waist represents the 632.8 nm exciting HeNe laser beam. If the raster scanned Au tip interacts with the near field of the nanostructure, the Au tip luminescence is excited. The luminescence signal is transmitted by a long-pass filter, blocking the excitation laser. Please note that in the used setup the detected luminescence signal is collected through the lens used to focus the exciting laser while the long pass filter is placed in front of the detector. The inset illustrates the spectral properties of the laser (green), the Au tip luminescence (red), and the long-pass filter transmittance (LPF, gray). SEM images of a typical tip and an aluminum oligomer are shown in (b) and (c).

image of such an Au tip with an apex radius of less than 10 nm is shown in Figure 1b, and the nanostructure is shown in Figure 1c. In order to adapt the polarization in the excitation focus to the radial symmetry of the heptamer, we utilize azimuthally and radially polarized cylindrical vector beams, here denoted as azimuthally/radially polarized doughnut modes (RPDM/APDM). When the APDM and the RPDM are focused through a high NA focusing element, they express very unique polarization conditions. The focal field of the APDM preserves the shape and the polarization of the collimated beam. The electric field component of the doughnut-shaped focus possesses an azimuthal polarization exclusively oriented in the sample plane with a diffraction-limited diameter of approximately  $\lambda$ . On the other hand, the focal field of the RPDM is dominated by a strong longitudinally polarized electric field component in the center of the focus, surrounded by a ring-shaped in-plane radially polarized field. The intensity ratio of the longitudinally to in-plane polarized field depends on the NA of the focusing element.<sup>19,20</sup> The all-in-plane polarization of the focal field of the APDM avoids the direct excitation of the upright oriented gold tip.

To exclude luminescence emitted by the nano-object itself, hence enhancing the signal-to-noise ratio of our method, we have selected aluminum as a material from which to fabricate the plasmonic nanostructures.<sup>21–25</sup> Aluminum is known to luminesce when excited in the UV region but not within the visible regime.<sup>26</sup> The plasmon resonances of aluminum nanostructures can usually be found at shorter wavelengths than for other coinage metals.<sup>27–29</sup> Our plasmonic nanostructure consists of seven aluminum disks with a height of 80 nm. The center disk possesses a diameter of 150 nm, and the six disks around are 140 nm in diameter while the spacing between them is 25 nm. As shown in Figure 2a,b, the outer disks of the

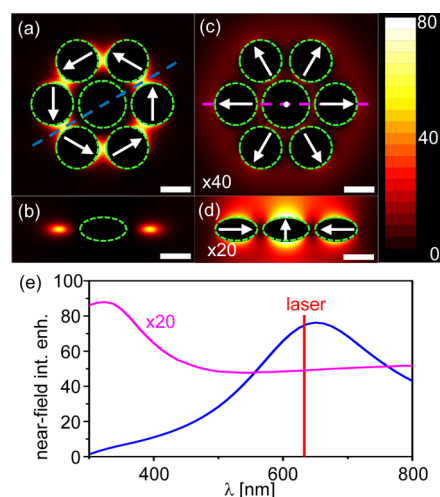


**Figure 2.** Simulated near-field intensity enhancement for the aluminum heptamer excited by a focused 632.8 nm APDM (a) and RPDM (c) represented in an  $xy$ -plane (focal plane) section through the center of the particles. The maximum of the intensity enhancement follows the polarization of the focal field and is located between the six particles in the ring by excitation with the APDM (a) or mainly above of the center disk at RPDM excitation (d). White arrows indicate the symmetry of the particles' dipolar moments. The location of the near-field intensity enhancement in the  $xz$ -plane along the blue line in (a) is shown in (b), while the  $xz$ -section of the radial case shown in (d) cuts through the center of three particles (c). The azimuthal near-field intensity enhancement has its maximum centered at 650 nm and a spectral width of around 300 nm (see blue line in (e)), while the radial near-field intensity enhancement maximum lies around 350 nm with a spectral width of  $\sim 200$  nm (see magenta line in (e)). Note that the radial calculations are enhanced with respect to the azimuthal cases by a factor of 40 (c) or 20 (d, e). The scale bars in (a)–(d) represent 100 nm.

oligomer are excited by the in-plane electric field component of the focus. We have calculated the modes of the oligomer and found that for the APDM the coupling of the six outer disks forms a plasmonic ring mode with a strongly red-shifted resonance at around 650 nm with a near-field intensity enhancement of at least 75. For the RPDM, the outer disks are excited radially and couple to the longitudinal mode of the center disk with a resonance at around 350 nm which can only be weakly excited with a HeNe laser of  $\lambda = 632.8$  nm. The simulations are performed using the surface integral method.<sup>30</sup>

The experiments to investigate the near-field imaging properties of the sharp gold tip were performed with a setup that was described previously in detail.<sup>31</sup> In brief, it consists of a combined home-built inverted confocal and scanning near-field optical microscope with RPDM/APDM illumination at a wavelength of 632.8 nm. These modes are formed by the method introduced by Dorn et al., utilizing a home-built four quadrant lambda half waveplate mode converter.<sup>32</sup> Excitation and detection are performed through a high numerical aperture (NA) oil immersion lens with an NA of 1.25. Elastic scattering is suppressed by a long-pass filter transmitting at  $\lambda > 641$  nm such that only Au luminescence is recorded.

A confocal image of the aluminum oligomer scanned through the focus of an APDM is shown in Figure 3e. No luminescence from the aluminum structure is detectable; neither was it found when excited with the RPDM. According to our simulations, we expect for excitation with the RPDM the strongest plasmon oscillation at the center disk with a polarization along the

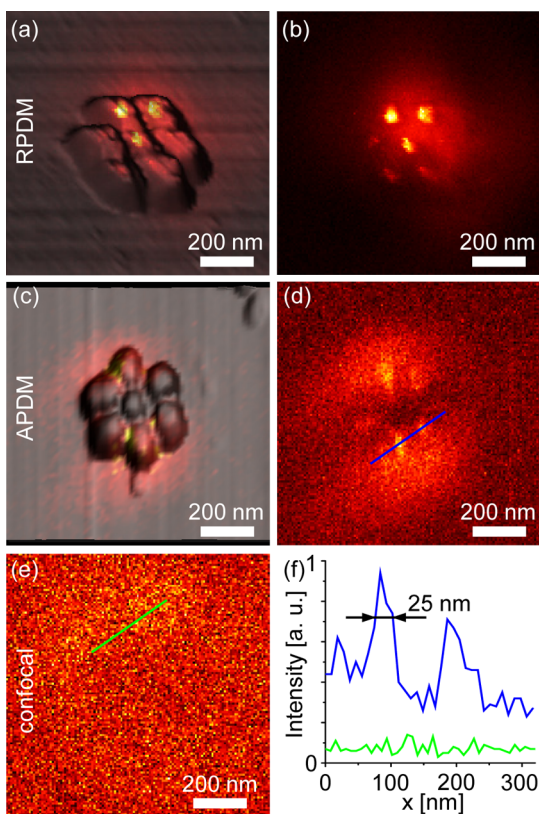


**Figure 3.** 3D topography overlaid by the locally excited Au tip luminescence image of the aluminum heptamer in the RPD (a) and APDM (c) focus while the Au tip luminescence images are shown in (b) for RPD and (d) for APDM. The Au tip luminescence images are in good agreement with the simulations in Figure 2. The luminescence signal (d) at tip positions inside of the gaps of the oligomer is at least twice as strong as the surrounding. The confocal scan image (e) of the same oligomer shows no traces of luminescence. (f) Line sections taken from (d) (blue) and the confocal image (e) (green). Please note that the Au tip luminescence data are acquired at the same heptamer but with different tips in different scanning directions.

optical axis, i.e., along the Au tip axis. Hence we expect an efficient coupling to the longitudinal plasmon of the Au tip and, indeed, observe strong luminescence from the tip apex when placed over the center disk. The strong luminescence signals of the upper disks in Figure 3a,b can be explained by a slight shift between the center of the RPD focus and the center of the heptamer.

For excitation with the APDM the plasmon oscillation of the Al disks is oriented in the sample plane, and therefore the regions with the highest optical near-field intensities are expected to be confined in the gaps between the disks, polarized parallel to the sample plane. Hence, efficient coupling to the Au tip plasmon occurs only when the tip apex is brought into the gaps between the disks. Figure 3f shows line sections taken from the tip luminescence (blue) and the confocal image (green). Both images were recorded with the same excitation power of  $150 \mu\text{W}$ . The confocal cross section depicts a steady background signal around 0.8 kcounts/s. The tip luminescence signal has a background of 3–4 kcounts/s and expresses some high features with 2.5 times higher luminescence intensity. These peaks exhibit a width of 25 nm, corresponding to the size of the gaps of two neighboring disks in the aluminum oligomer proving that the observed gold luminescence originates from

the tip's apex. The maximum signal-to-noise ratio for the radial case is 21 and for the azimuthal case 14. In the topography image in Figure 3c the gaps of the oligomer are clearly resolved. Here, the tip dips into the gaps between the individual particles, from where the luminescence signal in Figure 3d emerges. Comparing the luminescence intensities of the two polarizations, a 2 times higher intensity for radially polarized excitation can be observed. Here, the plasmon polarization of the center particle is oriented parallel to the main axis of the Au tip, leading to efficient energy transfer as depicted in Figure 4b.

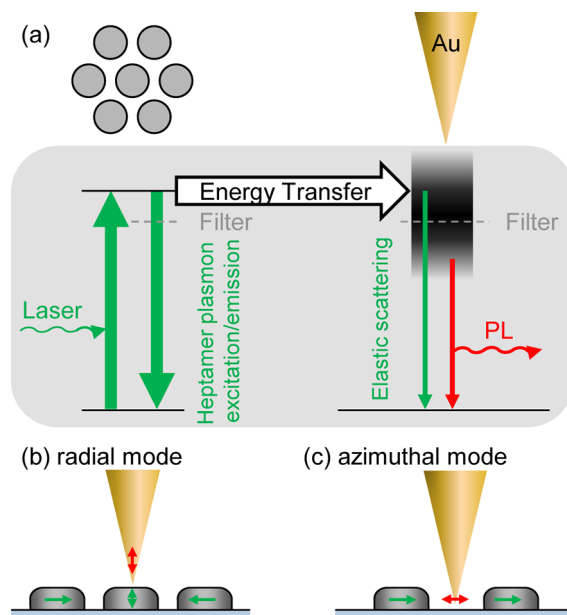


**Figure 4.** Sketch of the plasmonic coupling processes from the aluminum oligomer to the Au tip. (a) Coupled plasmon oscillations are excited in the oligomer with  $\lambda = 632.8 \text{ nm}$  irradiation. This energy is partly stored in the optical near field which enables energy transfer from the aluminum oligomer into the gold tip. The energy of the near field excites a defined plasmon oscillation in the tip, which can release its energy either via elastic scattering or via luminescence. The elastically scattered light is completely blocked by a long-pass filter in front of the detector. The two different coupling polarization configurations for radial and azimuthal illumination are shown in (b) and (c).

In the azimuthally excited Al oligomer the polarization of the particle plasmons and the main axis of the Au tip are perpendicular to each other, leading to a much weaker coupling (Figure 4c).

The energy transfer processes of the coupled system are schematically illustrated in Figure 4. The plasmonic system can be separated into two units, namely the aluminum heptamer and the gold tip, coupled by electromagnetic near-field interaction. On one hand, the plasmonic mode in the heptamer has a well-defined resonance near  $\lambda = 632.8 \text{ nm}$  (see Figure 2e), and its discrete energy level is represented by a thin horizontal line in the diagram. The gold tip, on the other hand, has no sharp plasmon resonance, hence acting more like a broadband antenna.<sup>33</sup> Therefore, its energy is portrayed as a broad gray-shaded area, illustrating that it can be excited by a range of wavelengths. Because of its nonresonant behavior, the excited tip will quickly relax, via either elastic scattering, photoluminescence, or nonradiatively via thermal losses.

The spectra of the heptamer's azimuthal plasmonic mode and the luminescence of the tip strongly overlap. However, the tip luminescence emission is strongly polarized in longitudinal direction, orthogonal to the heptamer's azimuthal mode. Hence, the latter cannot be significantly populated by the Au luminescence, and the coupling thus remains unidirectional.

Second, we look at the radial heptamer mode, where the polarization of the Au tip luminescence and the heptamer mode are indeed matching. However, the resonance of this mode is centered around 350 nm while the Au tip luminescence, with  $\lambda > 640$  nm, is too far away to achieve efficient coupling.

The nonresonant, dissipative behavior of the tip is an important prerequisite for its use as a near-field probe in the presented approach, leading to an effectively unidirectional transfer of energy from the heptamer to the tip and finally to the observed signal. This is reminiscent of the Förster resonance energy transfer (FRET) process, in which energy is unidirectionally transferred from a donor molecule to a rapidly decaying acceptor. Despite the strong near-field interaction between the two plasmonic units, the system remains in the weak-coupling regime. Consequently, the energy levels of the studied structure, i.e., the heptamer, are not influenced by the coupling to the probe, as would be expected for strongly coupled resonant systems.<sup>34</sup> In fact, the broadband response of the tip may even result in a larger PL signal than one would obtain with a resonant probe. As plasmonic modes on the tip can be excited efficiently for a range of wavelengths, our probe effectively enhances both, namely the excitation of electron-hole pairs at the laser wavelength as well as the PL signal upon recombination at a red-shifted wavelength. This 2-fold enhancement process is important for observing optical emission of very inefficient processes such as metallic photoluminescence.<sup>35</sup>

Experimentally, we have shown that the one-photon photoluminescence of a sharp Au tip can be used in a straightforward method to map the near field of coupled plasmonic systems. The spatial resolution of  $\leq 25$  nm allows us to visualize the ring-like coupling of an azimuthally excited aluminum oligomer. The energy transfer mechanism shows striking similarities to a FRET system. Many benefits of FRET as a sensor, including the built-in intensity reference given by the direct donor emission, are also available when using a gold tip as a near-field probe. Thus, a varying excitation efficiency of the nanostructure can be eliminated by observing the ratio of elastically to inelastically scattered light.

In summary, we have presented a way to map the optical near fields of plasmonic nanostructures with the luminescence of a sharp gold tip. Radially and azimuthally polarized illumination is used to match the symmetry of the investigated heptamer which is made of aluminum to exclude the luminescence of the structure itself. The energy transfer from the nanostructure to the gold tip is reminiscent of the FRET process, in which one dipole (donor) transfers its energy nonradiatively to another dipole (acceptor). As in FRET, the coupling efficiency depends not only on the spectral overlap of the donor emission to the acceptor absorption but also on other factors such as the correct orientation of the two systems with respect to each other.

Our technique is not limited to illumination with radially or azimuthally polarized doughnut modes (RPDM/APDM) and should, in principle, also work with different polarizations such as linear excitation. Because of the fixed position of the nano-object and the movement of the tip with respect to the focus,

luminescent materials like gold can also be investigated. Replacing the material with a luminescent one, however, cancels the advantage of the low background given by the aluminum structure. Additionally, different coupling states would have to be considered, making the interpretation of the data more sophisticated. These two extensions would further broaden the application scope of our method and will be the subject of future investigation.

## ■ ASSOCIATED CONTENT

### 📄 Supporting Information

Additional information with pure Au tip spectra excited by RPDM and APDM, an estimation of the quantum efficiency of the gold tip, the influence of the Au tip to the modes of the heptamer, and more measurement data with a note about the tip degradation. This material is available free of charge via the Internet at <http://pubs.acs.org>.

## ■ AUTHOR INFORMATION

### Corresponding Author

\*E-mail: [sebastian.jaeger@uni-tuebingen.de](mailto:sebastian.jaeger@uni-tuebingen.de) (S.J.); [alfred.meixner@uni-tuebingen.de](mailto:alfred.meixner@uni-tuebingen.de) (A.J.M.).

### Notes

The authors declare no competing financial interest.

## ■ ACKNOWLEDGMENTS

For image processing the WSXM Software of Nanotec was used.<sup>36</sup> Financial support by the "Kompetenznetz Funktionelle Nanostrukturen" of the Baden-Württemberg Stiftung as well as by DFG (ME 1600-5/2), ERC and BMBF is gratefully acknowledged.

## ■ REFERENCES

- (1) Davy, S.; Spajer, M. *Appl. Phys. Lett.* **1996**, *69* (22), 3306–3308.
- (2) Deeb, C.; Bachelot, R.; Plain, J.; Baudrion, A. L.; Jradi, S.; Bouhelier, A.; Soppera, O.; Jain, P. K.; Huang, L.; Ecoffet, C.; Balan, L.; Royer, P. *ACS Nano* **2010**, *4* (8), 4579–86.
- (3) Hubert, C.; Bachelot, R.; Plain, J.; Kostcheev, S.; Lerondel, G.; Juan, M.; Royer, P.; Zou, S. L.; Schatz, G. C.; Wiederrecht, G. P.; Gray, S. K. *J. Phys. Chem. C* **2008**, *112* (11), 4111–4116.
- (4) Hecht, B.; Sick, B.; Wild, U. P.; Deckert, V.; Zenobi, R.; Martin, O. J. F.; Pohl, D. W. *J. Chem. Phys.* **2000**, *112* (18), 7761–7774.
- (5) Michaelis, J.; Hettich, C.; Mlynek, J.; Sandoghdar, V. *Nature* **2000**, *405* (6784), 325–328.
- (6) Kühn, S.; Hettich, C.; Schmitt, C.; Poizat, J. P.; Sandoghdar, V. *J. Microsc.* **2001**, *202* (1), 2–6.
- (7) Kalkbrenner, T.; Ramstein, M.; Mlynek, J.; Sandoghdar, V. *J. Microsc.* **2001**, *202* (1), 72–76.
- (8) Haefliger, D.; Plitzko, J. M.; Hillenbrand, R. *Appl. Phys. Lett.* **2004**, *85* (19), 4466–4468.
- (9) Hillenbrand, R.; Knoll, B.; Keilmann, F. *J. Microsc.* **2001**, *202* (1), 77–83.
- (10) Bouhelier, A.; Beversluis, M. R.; Novotny, L. *Appl. Phys. Lett.* **2003**, *83* (24), 5041–5043.
- (11) Mooradian, A. *Phys. Rev. Lett.* **1969**, *22* (5), 185–187.
- (12) Boyd, G. T.; Yu, Z. H.; Shen, Y. R. *Phys. Rev. B: Condens. Matter* **1986**, *33* (12), 7923–7936.
- (13) Mohamed, M. B.; Volkov, V.; Link, S.; El-Sayed, M. A. *Chem. Phys. Lett.* **2000**, *317* (6), 517–523.
- (14) Fleischer, M.; Stanciu, C.; Stade, F.; Stadler, J.; Braun, K.; Heeren, A.; Haffner, M.; Kern, D. P.; Meixner, A. J. *Appl. Phys. Lett.* **2008**, *93* (11), 111114.
- (15) Huang, J. S.; Kern, J.; Geisler, P.; Weinmann, P.; Kamp, M.; Forchel, A.; Biagioni, P.; Hecht, B. *Nano Lett.* **2010**, *10* (6), 2105–10.

- (16) Dulkeith, E.; Niedereichholz, T.; Klar, T. A.; Feldmann, J.; von Plessen, G.; Gittins, D. I.; Mayya, K. S.; Caruso, F. *Phys. Rev. B* **2004**, *70* (20), 205424.
- (17) Tcherniak, A.; Dominguez-Medina, S.; Chang, W. S.; Swanglap, P.; Slaughter, L. S.; Landes, C. F.; Link, S. *J. Phys. Chem. C* **2011**, *115* (32), 15938–15949.
- (18) Sackrow, M.; Stanciu, C.; Lieb, M. A.; Meixner, A. J. *ChemPhysChem* **2008**, *9* (2), 316–320.
- (19) Züchner, T.; Failla, A. V.; Meixner, A. J. *Angew. Chem.* **2011**, *123* (23), 5384–5405.
- (20) Youngworth, K. S.; Brown, T. G. *Opt. Express* **2000**, *7* (2), 77–87.
- (21) Fan, J. A.; Wu, C.; Bao, K.; Bao, J.; Bardhan, R.; Halas, N. J.; Manoharan, V. N.; Nordlander, P.; Shvets, G.; Capasso, F. *Science* **2010**, *328* (5982), 1135–8.
- (22) Hentschel, M.; Saliba, M.; Vogelgesang, R.; Giessen, H.; Alivisatos, A. P.; Liu, N. *Nano Lett.* **2010**, *10* (7), 2721–6.
- (23) Lassiter, J. B.; Sobhani, H.; Fan, J. A.; Kundu, J.; Capasso, F.; Nordlander, P.; Halas, N. J. *Nano Lett.* **2010**, *10* (8), 3184–9.
- (24) Mirin, N. A.; Bao, K.; Nordlander, P. *J. Phys. Chem. A* **2009**, *113* (16), 4028–34.
- (25) Sancho-Parramon, J.; Bosch, S. *ACS Nano* **2012**, *6* (9), 8415–23.
- (26) Gryczynski, I.; Malicka, J.; Gryczynski, Z.; Nowaczyk, K.; Lakowicz, J. R. *Anal. Chem.* **2004**, *76* (14), 4076–81.
- (27) Chan, G. H.; Zhao, J.; Schatz, G. C.; Van Duyne, R. P. *J. Phys. Chem. C* **2008**, *112* (36), 13958–13963.
- (28) Langhammer, C.; Schwind, M.; Kasemo, B.; Zoric, I. *Nano Lett.* **2008**, *8* (5), 1461–71.
- (29) Blaber, M. G.; Arnold, M. D.; Harris, N.; Ford, M. J.; Cortie, M. B. *Physica B* **2007**, *394* (2), 184–187.
- (30) Kern, A. M.; Martin, O. J. *J. Opt. Soc. Am. A* **2009**, *26* (4), 732–40.
- (31) Hartschuh, A.; Qian, H.; Meixner, A. J.; Anderson, N.; Novotny, L. *Nano Lett.* **2005**, *5* (11), 2310–3.
- (32) Dorn, R.; Quabis, S.; Leuchs, G. *Phys. Rev. Lett.* **2003**, *91* (23), 233901.
- (33) Zhang, D.; Meixner, A. J. Book Chapter, Parabolic Mirror Assisted Gap-Mode Optical Ultramicroscopy. In *Handbook of Molecular Plasmonics*; Pan Stanford Publishing: Singapore, 2013; p 450.
- (34) Wang, H.; Brandl, D. W.; Nordlander, P.; Halas, N. J. *Acc. Chem. Res.* **2007**, *40* (1), 53–62.
- (35) Kern, A. M.; Meixner, A. J.; Martin, O. J. *ACS Nano* **2012**, *6* (11), 9828–36.
- (36) Horcas, I.; Fernandez, R.; Gomez-Rodriguez, J. M.; Colchero, J.; Gomez-Herrero, J.; Baro, A. M. *Rev. Sci. Instrum.* **2007**, *78* (1), 013705.